Journal of Taibah University for Science

ISSN: (Print) (Online) Journal homepage: https://www.tandfonline.com/loi/tusc20

On designing a sequential based EWMA structure for efficient process monitoring

Saddam Akber Abbasi, Qurat-Ul-Ain Khaliq, M. Hafidz Omar & Muhammad Riaz

To cite this article: Saddam Akber Abbasi, Qurat-Ul-Ain Khaliq, M. Hafidz Omar & Muhammad Riaz (2020) On designing a sequential based EWMA structure for efficient process monitoring, Journal of Taibah University for Science, 14:1, 177-191, DOI: 10.1080/16583655.2020.1712011

To link to this article: https://doi.org/10.1080/16583655.2020.1712011

Published online: 16 Jan 2020.

JOURNAL OF TAIBAH UNIVERSITY FOR SCIENCE
2020, VOL. 14, NO. 1, 177–191
https://doi.org/10.1080/16583655.2020.1712011

JTUSCI

Journal of Taibah University for Science

Taylor & Francis
Taylor & Francis Group

RESEARCH ARTICLE

OPEN ACCESS Check for updates

On designing a sequential based EWMA structure for efficient process monitoring

Saddam Akber Abbasi [a], Qurat-Ul-Ain Khaliq [b], M. Hafidz Omar[c] and Muhammad Riaz [c]

[a]Department of Mathematics, Statistics and Physics, Qatar University, Doha, Qatar; [b]Department of Statistics, Allama Iqbal Open University, Islamabad, Pakistan; [c]Department of Mathematics and Statistics, King Fahd University of Petroleum and Minerals, Dhahran, Saudi Arabia

ABSTRACT

Control chart is a popular technique that is widely used in statistical process control to identify any possible deviations from a stable state of a process. Shewhart charts are famous for identifying larger shifts, while cumulative sum and exponentially weighted moving average control charts are well known for identifying smaller shifts in process parameters. This study examines the performance of a sequential-based EWMA (namely SEWMA$_{\beta}$) chart for observing the location of a normally distributed process. The performance of SEWMA$_{\beta}$ is oberved by using several overall run length properties (like average, median and standard deviation). The comparative study reveals that the overall performance of the proposed design is better than the existing counterparts. Moreover, the superiority depends on the choice of the design parameters of the proposed chart. A real-life data set from a steel rod manufacturing industry were considered to show the real-life illustration of the proposed design.

ARTICLE HISTORY
Received 5 August 2019
Revised 4 December 2019
Accepted 29 December 2019

KEYWORDS
Average run length; control charts; exponentially weighted moving average; sequential approach; manufacturing processes

1. Introduction

Statistical process control (SPC) is a mechanism that helps in monitoring the stability of an ongoing process to produce quality products. It comprises extremely powerful tools such as pareto chart, cause and effect diagram, fishbone diagram, flow diagram and control chart (cf. Montgomery [1]). SPC is vital for the reputation of a manufacturing industry that relies on the quality of products in a global market competition. Within the SPC toolkit, control charts are the most important tools used for observing and detecting the special cause variations and ultimately enhancing the performance of the product (cf. Shewhart [2]). In order to monitor any ongoing process, the use of apropriate control charting techniques is essential to ensure the stability of the process and to provide several benefits such as reduction in cost and time and increase in efficiency of the industrial process. Shewhart charts are well known for the detection of large shifts in process parameters while exponentially weighted moving average (EWMA) (cf. Roberts [3]) and cumulative sum (CUSUM) charts (cf. Page [4]) are mostly used for the detection of small to moderate shifts. In this study, we introduce an efficient sequential-based EWMA chart which is more sensitive to shifts in process location. Several authors worked to enhance the performance of classical EWMA chart (cf. Yang et al. [5]). The aim of this article is to design an EWMA chart based on a sequential testing algorithm to enhance the performance of the traditional EWMA chart and to increase its efficiency over the classical setup.

In the existing literature, there are mainly two forms of charts where sequential process monitoring is used. That is, some SPC practitioners adopt sequential sampling in their study, while others implement SPRT control charts for online monitoring. Both approaches have an advantageous mechanism for quality control charts for the monitoring of process parameters. According to Matheson [6], the probability of identifying the shift using sequential sampling is more than or equivalent to the likelihood of identifying the shift using a random sampling technique in-control charts as it needs fewer number of samples at a smaller cost. Green [7] highlighted that there is little advantage to sequential sampling if the cost of sample collection is similar to the cost of sample analysis. That is, if sequential sampling is to be more economical than many used approaches, less time should be needed to take a sample in the field than to analyse it in the laboratory. Sequential sampling is appropriate when the time required to gather at least one observation is a very small interval. In this way, it is likely to take numerous samples successively at a sampling point. A useful discussion in this context may be seen in Green [8] and the references therein. As a natural extension of the ideas from sequential analysis, sequential sampling methods have been widely used in the area of acceptance sampling but not so much in process monitoring (cf. Stoumbos and Reynolds [9, 10]).

The sequential probability ratio test (SPRT) chart is useful where testing is very costly or difficult. Peng and Reynolds [11] applied sequential sampling using gen-

CONTACT Saddam Akber Abbasi sabbasi@qu.edu.qa

eralized likelihood ratio (GLR) charts. Steiner at el. [12] designed the exact expression for the Wald-SPRT and CUSUM design. Various authors also worked on single directional process monitoring using sequential sampling (SS). Reynolds [13–15] and Reynolds et al. [16, 17] designed sequential sampling-based control charts which were very effective for detecting changes in a single direction in the process, with some tuning parameters specified. Reynolds and Arnold [18] constructed a one-sided EWMA design for VSI following a sequential sampling algorithm. Zhang et al. [19] designed an EWMA chart under a sequential sampling scheme for single directional process monitoring, and this design was more sensitive to single direction shift detection in the process. Stoumbos and Reynolds [20] designed SPRT chart for process location which was more efficient and highly effective with administrative benefits. Ou at el. [21] designed an SPRT location chart using several sampling intervals. Ou at el. [22] further enhanced the performance of SPRT location chart. Xu and Jeske [23] used SPRT technique to deal with the INAR model. Godase and Mahadik [24] introduced an SPRT dispersion chart.

Keeping in view of several dynamic aspects of SPRT and sequential sampling, we intend to design a sequential algorithm-based EWMA chart, named SEWMA$_{\beta}$. This scheme uses two pairs of control limits as follows in SPRT. The novelty of this article is to propose a more flexible EWMA control chart for monitoring the process location by employing an SPRT decision algorithm. The rest of this paper is organized as follows: Section 2 provides the design structure of the proposed sequential EWMA chart. Section 3 demonstrates procedural flow for the computation of run length measures. The performance evaluation and comparative analysis are provided in Section 4. A real-life application concerning the monitoring of breaking strength of steel rods is presented in Section 5. Finally, Section 6 lists the main finding and recommendations of the study.

2. Design structure of the proposed SEWMA$_{\beta}$ chart

This section provides the design structure of the proposed chart. For the rest of the current article, we will denote the proposed chart as a SEWMA$_{\beta}$ chart. In the SPRT technique, observations are taken in groups of one or more observations. If the single observation falls in an indecision zone then another observation is taken until a decision is achieved. For the sake of simplicity, we have used individual observations for this study; however, subgroups of different sizes may also be considered on similar lines (cf. Wald [25]).

Let $X_1, X_2, X_3 \ldots \ldots \ldots \ldots, X_n$ be a set of independent individual observations, selected from a specific probability distribution (say normal distribution). An individual observation may be classified into three non-overlapping regions categorized as

Region I: the acceptance region (where the process is considered to be in-control);

Region II: the resampling region (where the process needs to be resampled);

Region III: the rejection region (where the process is considered to be out-of-control).

For a single observation, let α be the probability of falling in the rejection region and γ be the probability of falling in the indecision region. Then under a resampling setup, the respective probabilities for the three regions are given as shown in Figure 1.

Let us denote R_s as the resampling region. Now based on observed sample values X_{js} we may define a plotting statistic, say Z_j, of the SEWMA$_{\beta}$ chart as follows:

$$Z_j = \lambda_g I_j + (1 - \lambda_g) Z_{j-1}, \quad j = 0, 1, 2, \ldots, \tag{1}$$

where $E[Z_0] = \mu_0$ and $0 < \lambda_g \leq 1$. Also for compactness, we can alternatively denote I_j as follows:

$$I_j = \begin{cases} X_j & \text{if } X_j \notin R_s \\ X_j + \sum_{k=1}^{N_j} Y_{j,k} & \text{if } Z_j \in R_{s'} \end{cases} \tag{2}$$

where N_j is the number of data points sequentially sampled in the jth monitoring batch, k is just the counter for the sequential sampling, and $Y_{j,k}$ is the resampled point in the kth sequence of the jth monitoring batch. Or alternatively, we can denote I_j as

$$I_j = X_j + \sum_{k=0}^{N_j} Y_{j,k}, \text{ when } X_j \notin R_s.$$

We note that the probability of a sample $Z_j \in R_s$ is given by $P(Z_j \in R_s) = \gamma$. Samples will be drawn at each stage j until $Z_j \notin R_s$. Moreover, for simplicity of derivations and for finding the first two centred moments of Z_j, we will use the transformation $\lambda_g^* = 1 - \lambda_g$(check Appendix for details). It is to be mentioned that λ_g is the smoothing or the weighting factor $(0 < \lambda_g \leq 1)$ and it may take varying values depending on how frequently the monitoring statistic is falling in the indecision region. In other words, it may be used to cater to the sensitivity of the shifts that might occur in a process. The initial value of **SEWMA$_{\beta}$** statistic is usually set to be $Z_0 = \mu_0$. Moreover, X and Y are independently distributed random variables that follow the normal distribution with μ_0 as mean and variance σ_0^2.

The mean and variance of SEWMA$_{\beta}$ statistic are

$$\left.\begin{aligned} \mu_{Z_i} &= \mu_0 \left(1 + \tfrac{1}{1-\gamma}\right) \\ \sigma_{Z_i}^2 &= \left(1 + \tfrac{1}{1-\gamma}\right)\left(\tfrac{1-\lambda_g^*}{1+\lambda_g^*}\right)\sigma_0^2 + \tfrac{\gamma}{(1-\gamma)^2}\left(\tfrac{1-\lambda_g^*}{1+\lambda_g^*}\right)\mu_0^2 \end{aligned}\right\}. \tag{3}$$

It is to be mentioned that the abovementioned expressions are asymptotic versions of mean and variance of

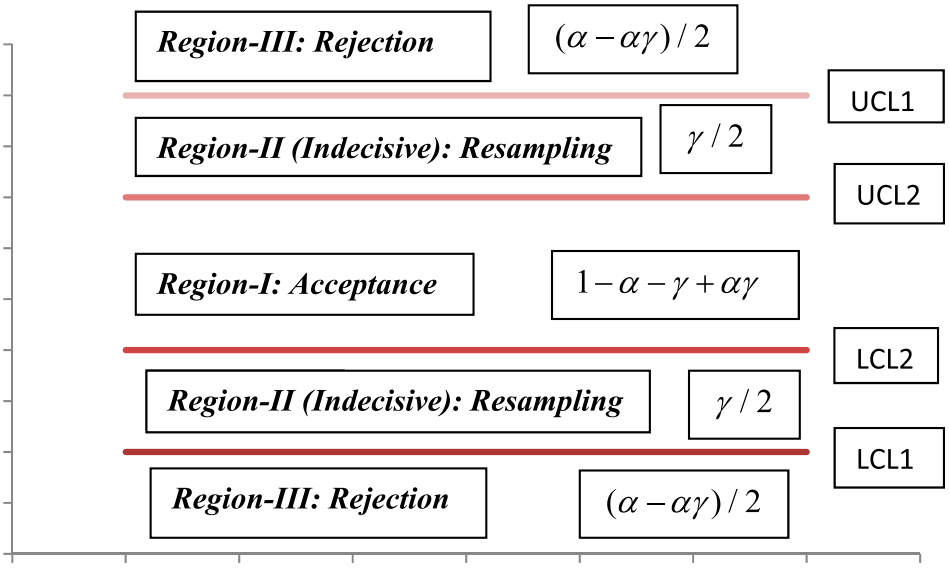

Figure 1. A graphical display of decision regions under sequential algorithm.

Z_j (cf. Appendix). The details regarding the derivations of these expressions can be seen in the Appendix.

The control limits of the proposed SEWMA$_\beta$ control chart are in the form of two pairs of upper and lower control limits because of the three regions (as indicated in Figure 1). Using the expressions given in Equation (3) and the splitted regions in Figure 1, the control limits of the proposed SEWMA$_\beta$ chart are defined as

$$\left.\begin{aligned} \text{LCL}_2 &= \mu_{Z_j} - L_2\sigma_{Z_j} \\ \text{UCL}_2 &= \mu_{Z_j} + L_2\sigma_{Z_j} \\ \text{LCL}_1 &= \mu_{Z_j} - L_1\sigma_{Z_j} \\ \text{UCL}_1 &= \mu_{Z_j} + L_1\sigma_{Z_j} \end{aligned}\right\}, \tag{4}$$

where LCL_1, UCL_1 determine the out-of-control and LCL_2, UCL_2 determine the in-control regions, respectively, and accordingly the inner region (i.e. the area between UCL_1 & UCL_2 and LCL_1 & LCL_2) corresponds to the indecision region where we need to resample (cf. Figure 1). It is to be mentioned that when the monitoring statistic falls in the indecision region, we continue resampling and keep updating the plotting statistic (using the new sample information) until it falls in one of the decisive regions (i.e. Regions I or III). The quantities L_1 and L_2 are the control limit coefficients that are used to adjust the in- and out-of-control limits to achieve the desired in-control average run length (denoted by ARL_0). These coefficients must hold the condition that $L_1 \geq L_2$. Note that for $L_1 = L_2$, the performance of SEWMA$_\beta$ chart is exactly the same as the usual EWMA chart.

i. Percentile Adjustment for Indecision zone

In the sequential sampling setup, it is important to adjust the indecision zone in order to achieve the desirable properties corresponding to a prespecified ARL_0. In this study, we adjust the width of the indecision region, according to the following relation

$$L_2 = L - \beta L, \tag{5}$$

where L is the control limit coefficient (at a prespecified ARL_0) for the SEWMA$_\beta$ chart, which matches its performance with the EWMA chart (i.e. $L_1 = L_2 = L$), and β is the factor used to adjust the width of the decisive zone, $0 \leq \beta \leq$. For $\beta = 0$, $L_1 = L_2 = L$, the performance of the SEWMA$_\beta$ chart is exactly the same as the proposed SEWMA$_\beta$ chart.

2.1. Decision criteria

Using Equations (3)–(6), we compute the two pairs of control limits for a fixed ARL_0. For each new monitoring sample, we calculate the plotting statistic Z_j using Equation (1) sequentially. If the plotting statistic Z_j falls in one of the decisive regions I or III, then we make the decision accordingly. If Z_j falls in the indecision region, we continue resampling to update the plotting statistic (using the new sample information), until it falls in one of the decisive regions (i.e. Regions I or III). Figure 2 provides an exemplary charting display for the proposed SEWMA$_\beta$ chart.

It is to be noted that: (i) the sensitivity of the regions may be controlled by the design parameters, namely λ_g, β, L_1 and L_2; (ii) for the sake of simplicity, we have used $\lambda_g = \lambda$ for each occasion where we needed to resample; (iii) classical EWMA chart is a special case of the proposed chart when $L_1 = L_2 = L$.

3. Performance evaluation techniques

To assess the performance of the SEWMA$_\beta$ chart, we have used different run length properties, such as the average (ARL), the median (MRL) and the standard deviation of the run length (SDRL) distribution. ARL is the

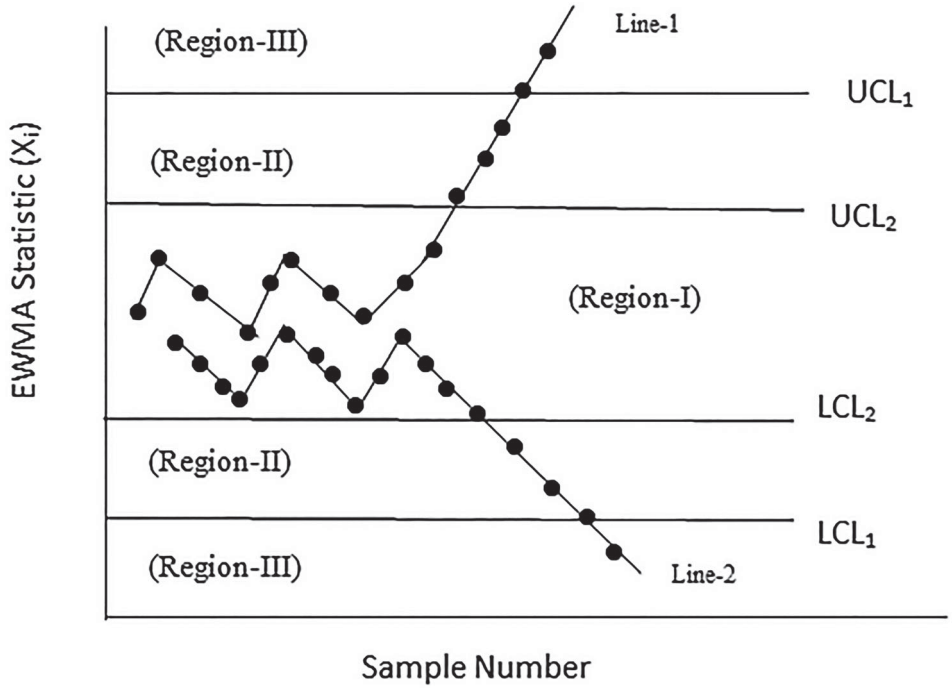

Figure 2. A charting display for the SEWMA$_{\beta}$ control chart.

frequently used measure to evaluate the performance of control charts. ARL can be categorized into in-control (IC) average run length (ARL$_0$) and out-of-control ARL (ARL$_1$), defined as

ARL$_0$: Average number of samples plotted on a control chart *until the first* point goes **outside** the limits, when the process is *in-control* (IC).

ARL$_1$: Average number of samples plotted on a control chart *until the first* point goes **out** of the limits, when the process is *out-of-control* (OOC).

Similarly, MRL and SDRL can be defined based on an in-control or out-of-control state of the process.

To examine the detection ability of the SEWMA$_{\beta}$ chart, shifts are introduced in the in-control (IC) process location say, μ_0 and the OOC process mean level is defined as $\mu_1 = \mu_0 + \delta\sigma_0$, where δ refers to the amount of shift.

These run length properties may be calculated by using the following expressions (cf. Chakraborti [26], Khaliq et al.[27])

$$\text{ARL} = \text{Expected}\,(RL) = \int_{-\infty}^{+\infty} (RL) f(RL) d(RL). \quad (6)$$

$$\text{SDRL} = \sqrt{E(RL^2) - [E(RL)]^2}. \quad (7)$$

$$\text{MRL} = p(RL \leq m) = p(RL > m) = \int_{-\infty}^{m} f(RL) d(RL) = 0.5. \quad (8)$$

3.1. Algorithm for SEWMA$_{\beta}$ chart construction

In this subsection, we discuss how to construct the SEWMA$_{\beta}$ chart via an algorithm. The following are the necessary steps of the algorithm to achieve this work.

(i) Draw a random observation from a normal distribution with in-control mean μ_0 and standard deviation σ_0. Without loss of generality, we used $\mu_0 = 0$ and $\sigma_0 = 1$. Find the monitoring statistic for the SEWMA$_{\beta}$ chart (using Equation (1)).
(ii) Select $L_1 = L_2 = L$ and plot the monitoring statistic (using the criterion mentioned in (2)) against the control limits (given in Equation (4)), to achieve the desired IC-ARL$_0$.
(iii) Decide L_2 using Equation (5) after selecting a level of p. For a given specified L_2, $L_1$is then chosen to achieve the desired ARL$_0$.

We now discuss the simulation procedure to assess the performance of the SEWMA$_{\beta}$ chart.

3.2. Algorithm for RL properties

Monte Carlo simulations are used to obtain the RL properties of the SEWMA$_{\beta}$ chart, following Quesenberry [28] and Khaliq at el.[29]. The steps taken in the simulation study are as follows.

(i) With the sequential charting algorithm described in the previous subsection, construct the SEWMA$_{\beta}$ chart.
(ii) For getting out-of-control RL, shifts are introduced in the process mean level by plotting the monitoring statistic of the shifted samples against the control limits (using the criterion mentioned in Equation (2)). The OOC run length is computed as

the number of samples plotted on the control chart before the first point goes beyond LCL2 or UCL2.

(iii) The process is repeated 100,000 times to record RL values of the proposed design.

(iv) Using the RL's from step (iii) above, the ARL, MRL and SDRL are computed as the mean, median and standard deviations of these RLs respectively.

4. Performance evaluation and comparisons

In this section, we evaluate the performance of the proposed SEWMA$_{\beta}$ chart at different levels of design parameters λ, β, and ARL_0, L_1 and L_2. The performance of the proposed SEWMA$_{\beta}$ chart is compared with some existing charts for efficient detection of shifts in the process mean level. Tables 1–3 provide the RL properties of the proposed SEWMA$_{\beta}$ chart and the competing charts such as EWMA, CUSUM and FIR-EWMA charts for varying values of λ, β and δ. Moreover, Figures 1 and 2 provide a graphical comparison of the performance of the proposed SEWMA$_{\beta}$ chart at varying levels of design parameters.

4.1. SEWMA$_{\beta}$ performance analysis

This section is about the *Run Length* (*RL*) performance of *SEWMA*$_{\beta}$ chart by varying β and λ. Several performance measures were used to observe the performance of the proposed design, i.e. average, median and standard deviation (cf. *ARL, MRL* and *SDRL*). Tables 1 and 2 represent the ARL_1, *MRL* and *SDRL* performance of SEWMA$_{\beta}$ versus EWMA chart by varying λ and β. Here, λ is the smoothing or weighting factor that has a similar effect on the performance of the EWMA chart. The β has a significant impact on the performance of the SEWMA$_{\beta}$ chart. Here, β is control limits adjusting factor (percentile) and it guarantees the better ARL_1 performance of SEWMA$_{\beta}$ chart. Several choices of β are 2%, 4%, 6%, 8%, 10% and 12%. It may be observed from the tables that we have smaller ARL_1, *MRL* and *SDRL* values from SEWMA$_{\beta}$ than classical EWMA.

i. ARL_1 Performance Analysis

Although both designs performed equally well based on the ARL under the in-control situation, our proposed design has better $\boldsymbol{ARL_1}$ performance in the out-of control situations than the classical EWMA chart as it has smaller $\boldsymbol{ARL_1}$ for all choices of β. As an illustration, consider Table 2; EWMA chart shows $ARL_1 = 282$ while SEWMA$_{\beta}$ at $\beta = 2\%, 4\%, 6\%, 8\%, 10\%$ and 12% are 272.51, 264.29, 256.36, 173.4, 232.68 and 271, respectively, for $\lambda = .9$ and $\delta = .2$. That is, SEWMA$_{\beta}$ charts have better ARL_1 than classical EWMA chart. This performance gain may be observed up to a process shift of $\delta = 4$. Similar ARL behaviour may be observed from Tables 1 and 2. Figures 3 and 4 also support these results.

ii. MRL Performance Analysis

SEWMA$_{\beta}$ not only have better $\boldsymbol{ARL_1}$ but it also performed well considering median RL properties. EWMA and SEWMA$_{\beta}$ are equally efficient at $\beta = 5\%$. However, our design has smaller MRL values for small to moderate shift at $\beta = 4\%, 6\%, 8\%, 10\%$, and 12%. Consider Table 2. The MRL values of EWMA is 282.14 while for SEWMA$_{\beta}$, MRL values are 272.51 (2%), 264.29 (4%), 256.36 (6%), 173.4 (8%), 232.68 (10%) and 217.25 (12.5%). Furthermore, it may be observed from Tables 1 and 2, our proposed design showed better MRL values up to shift of $\delta = 1.75$ at $\lambda = 0.99, 0.5, 0.25$ and 0.05.

iii. SDRL Performance Analysis

SEWMA$_{\beta}$ has smaller SDRL values than EWMA up to $\delta = 3$. SEWMA$_{\beta}$ outperformed the EWMA chart at $\lambda = 0.99, 0.5, 0.25$ and 0.05 up to $\delta = 3$. As an example, consider Table 2. For $\delta = .25$, our proposed design showed *SDRL* values of 273.04 (2%), 261.04 (4%), 252.04 (6%), 171.883 (8%), 227.37 (10%) and 214.32 (12.5%) while EWMA showed *SDRL* of 282.14. Similar *SDRL* behaviour may be observed from Tables 1 and 2. That is, our proposed design has a smaller variation in *RL* than the classical EWMA design.

4.1.1. General Comments

The proposed SEWMA$_{\beta}$ chart has better *ARL*, *MRL* and *SDRL* performance than the classical EWMA design. The proposed design is more efficient than the classical one from small, moderate and larger shifts. In particular, SEWMA$_{\beta}$ is more efficient than the EWMA chart when $\beta > 0.02$ as may be seen in Figures 3 and 4. It is to be noted that the SEWMA$_{\beta}$ reduces to the EWMA chart when $\beta = 0$.

4.2. Comparative analysis of SEWMA$_{\beta}$ versus EWMA, CUSUM and FIR-EWMA

This section is designed to show the comparative performance of SEWMA$_{\beta}$ versus classical EWMA, CUSUM and FIR-EWMA chart using several ARL_0 values. Table 3 demonstrates the ARL performance of SEWMA$_{\beta}$ ($\beta = 10\%$ and 12.5%) against classical EWMA and CUSUM design at $ARL_0 = 168, 400$ and 500. Moreover, Table 3 also presents the *ARL* performance of SEWMA$_{\beta}$ ($\beta = 10\%$ and 12.5%) versus FIR-EWMA at ARL_0. The findings are as discussed below.

***i.* SEWMA$_{\beta}$ versus EWMA and CUSUM charts at $\boldsymbol{ARL_0 = 168, 400}$ and 500.**

Table 3 shows the *ARL* performance of SEWMA$_{\beta}$ versus EWMA and CUSUM charts using $ARL_0 = 168$, 400 and 500. It may be perceived that SEWMA$_{\beta}$ has smaller ARL_1 values than EWMA until a shift parameter of $\delta = 2$ while it has better performance than CUSUM up to $\delta = 1.5$. SEWMA$_{\beta}$ chart ($\beta = 10\%$ and 12.5%) has

Table 1. RL properties of SEWMA$_{\beta}$ and EWMA ($L_1 = L_2$) charts for varying δ and β when $\lambda = 0.05$ and 0.25 at ARL$_0 = 370$.

		$\lambda = 0.05$							$\lambda = 0.25$						
	β	**0**	**0.02**	**0.04**	**0.06**	**0.08**	**0.1**	**0.125**	**0**	**0.02**	**0.04**	**0.06**	**0.08**	**0.1**	**0.125**
	L_1	**0.2928**	**0.2952**	**0.2989**	**0.304**	**0.3117**	**0.3204**	**0.3318**	**0.9251**	**0.9427**	**0.9669**	**1.0075**	**1.0561**	**1.1222**	**1.227**
	L_2	**0.2928**	**0.2869**	**0.2811**	**0.2752**	**0.2694**	**0.2636**	**0.2563**	**0.9251**	**0.9066**	**0.888**	**0.8695**	**0.851**	**0.8325**	**0.8095**
0	**ARL**	371.38	370.8	370.47	369.01	371.78	369.66	369.61	368.71	370.45	369.58	370.86	370.32	370.44	370.86
	MDRL	259	261	260	259	263	262	259	257	257	257	258	256	258	256
	SDRL	360.39	358.6	358.72	355.76	358.61	355.81	358.91	371.03	370.79	366.47	366.82	363.78	366.12	363.87
0.25	**ARL**	73.46	72.69	71.97	71.06	70.36	68.92	66.96	136.64	134.36	130.2	127.72	122.64	117.24	109.89
	MDRL	56	55	55	54	53	52	50	95	93	89	87.5	84	81	76
	SDRL	59.34	58.46	57.86	57.45	56.84	55.72	54.3	133.78	131.71	129	126.45	120.19	114.6	106.85
0.5	**ARL**	26.61	26.24	25.89	25.41	24.91	24.33	23.54	41.05	39.77	38.29	36.95	35.2	33.42	31.19
	MDRL	23	22	22	22	21	21	20	30	29	28	27	26	25	23
	SDRL	15.54	15.34	15.11	14.9	14.72	14.32	13.98	36.62	35.32	33.69	32.88	31.16	29.18	27.29
0.75	**ARL**	15.38	15.14	14.87	14.58	14.25	13.94	13.52	18.13	17.48	16.89	16.31	15.57	14.86	13.92
	MDRL	14	14	14	13	13	13	12	14	14	13	13	12	11	11
	SDRL	6.96	6.87	6.76	6.74	6.58	6.48	6.3	14.15	13.53	13.08	12.63	11.99	11.46	10.57
1	**ARL**	10.75	10.56	10.36	10.17	9.91	9.7	9.42	10.26	9.95	9.6	9.25	8.92	8.54	8.11
	MDRL	10	10	10	9	9	9	9	8	8	8	8	7	7	7
	SDRL	4.01	3.99	3.93	3.88	3.82	3.79	3.69	6.81	6.57	6.32	6.03	5.79	5.53	5.16
1.25	**ARL**	8.29	8.14	7.96	7.8	7.63	7.46	7.23	6.9	6.72	6.52	6.31	6.09	5.9	5.63
	MDRL	8	8	8	7	7	7	7	6	6	6	5	5	5	5
	SDRL	2.69	2.66	2.63	2.6	2.55	2.54	2.47	3.86	3.77	3.64	3.5	3.38	3.26	3.07
1.5	**ARL**	6.76	6.63	6.5	6.37	6.22	6.07	5.93	5.19	5.04	4.9	4.77	4.62	4.48	4.31
	MDRL	6	6	6	6	6	6	6	5	5	4	4	4	4	4
	SDRL	1.97	1.94	1.9	1.89	1.86	1.82	1.8	2.5	2.42	2.35	2.25	2.18	2.11	2.02
1.75	**ARL**	5.73	5.61	5.51	5.4	5.27	5.17	5.02	4.14	4.03	3.93	3.82	3.73	3.62	3.49
	MDRL	6	5	5	5	5	5	5	4	4	4	4	3	3	3
	SDRL	1.53	1.51	1.48	1.47	1.45	1.43	1.38	1.75	1.71	1.66	1.61	1.57	1.52	1.48
2	**ARL**	4.99	4.89	4.8	4.7	4.61	4.51	4.39	3.45	3.38	3.31	3.23	3.15	3.07	2.97
	MDRL	5	5	5	5	4	4	4	3	3	3	3	3	3	3
	SDRL	1.23	1.21	1.19	1.18	1.17	1.15	1.12	1.31	1.28	1.26	1.24	1.2	1.17	1.13
2.5	**ARL**	3.99	3.91	3.83	3.75	3.69	3.62	3.53	2.65	2.59	2.54	2.49	2.44	2.38	2.32
	MDRL	4	4	4	4	4	4	3	3	2	2	2	2	2	2
	SDRL	0.88	0.85	0.84	0.84	0.82	0.82	0.81	0.85	0.83	0.82	0.81	0.8	0.78	0.77
3	**ARL**	3.36	3.3	3.24	3.17	3.11	3.05	2.97	2.2	2.15	2.11	2.07	2.02	1.98	1.94
	MDRL	3	3	3	3	3	3	3	2	2	2	2	2	2	2
	SDRL	0.66	0.66	0.65	0.65	0.65	0.64	0.64	0.62	0.61	0.6	0.6	0.6	0.6	0.59
3.5	**ARL**	2.91	2.85	2.81	2.76	2.71	2.65	2.59	1.89	1.86	1.82	1.78	1.74	1.71	1.66
	MDRL	3	3	3	3	3	3	3	2	2	2	2	2	2	2
	SDRL	0.56	0.56	0.57	0.57	0.57	0.57	0.56	0.52	0.53	0.53	0.54	0.54	0.54	0.54
4	**ARL**	2.57	2.52	2.48	2.43	2.39	2.34	2.28	1.67	1.63	1.59	1.56	1.52	1.48	1.43
	MDRL	3	3	2	2	2	2	2	2	2	2	2	2	1	1
	SDRL	0.53	0.53	0.52	0.52	0.5	0.49	0.46	0.51	0.51	0.51	0.51	0.51	0.51	0.5

Table 2. RL properties of SEWMA$_{\beta}$ and EWMA ($L_1 = L_2$) charts for varying δ and β when $\lambda = 0.50$ and 0.99 at ARL$_0 = 370$.

		$\lambda = 0.50$							$\lambda = 0.99$						
	β	**0**	**0.02**	**0.04**	**0.06**	**0.08**	**0.1**	**0.125**	**0**	**0.02**	**0.04**	**0.06**	**0.08**	**0.1**	**0.125**
	L_1	**1.7176**	**1.7580**	**1.8146**	**1.9001**	**2.0317**	**2.2014**	**2.4699**	**4.1691**	**4.2553**	**4.3970**	**4.6444**	**4.7667**	**5.4866**	**6.2954**
	L_2	**1.7176**	**1.6836**	**1.6489**	**1.6148**	**1.5802**	**1.5461**	**1.5028**	**4.1691**	**4.0857**	**4.0024**	**3.9190**	**3.8356**	**3.7522**	**3.6480**
0	**ARL**	370.65	369.53	369.36	369.16	369.29	368.68	370.45	370.61	369.68	368.47	371.67	369.97	370.94	371.45
	MDRL	262.00	258.00	255.00	255.00	254.00	253.00	257.50	259.00	255.00	256.00	257.00	254.00	256.00	259.00
	SDRL	370.48	368.88	366.84	365.94	367.20	373.17	371.90	371.57	373.98	367.22	371.72	370.87	371.43	373.03
0.25	**ARL**	195.37	190.57	182.94	176.81	169.27	160.20	148.79	282.14	272.51	264.29	256.36	173.40	232.68	217.25
	MDRL	136.00	131.00	126.00	122.00	117.00	112.00	102.00	194.00	187.00	182.00	178.00	119.00	165.00	152.00
	SDRL	193.04	190.75	183.04	175.05	166.64	156.53	147.47	283.21	273.04	261.83	252.56	171.83	227.37	214.32
0.5	**ARL**	70.89	67.59	63.89	60.33	56.75	52.38	46.50	155.53	144.39	135.22	125.01	58.32	103.21	88.90
	MDRL	49.00	47.00	45.00	42.00	39.00	37.00	33.00	108.00	100.00	95.00	87.00	41.00	71.00	61.00
	SDRL	69.40	65.56	61.68	58.37	55.13	50.14	44.84	153.73	142.99	132.96	125.10	56.48	102.76	89.22
0.75	**ARL**	30.29	28.75	26.86	25.05	23.32	21.60	19.43	80.65	73.82	67.25	61.11	24.11	48.56	41.35
	MDRL	22.00	21.00	19.00	18.00	17.00	16.00	14.00	57.00	52.00	47.00	42.00	17.00	34.00	29.00
	SDRL	28.35	26.37	24.68	22.87	20.96	19.49	17.39	78.88	72.76	65.99	60.02	21.78	47.51	40.40
1	**ARL**	15.27	14.42	13.63	12.80	11.98	11.21	10.19	44.02	39.56	35.45	32.15	12.28	25.35	21.81
	MDRL	11.00	11.00	10.00	10.00	9.00	8.00	8.00	31.00	28.00	25.00	23.00	9.00	18.00	15.00
	SDRL	13.02	12.37	11.55	10.83	10.09	9.41	8.53	43.31	38.50	34.29	31.00	10.34	24.70	21.08
1.25	**ARL**	8.89	8.48	8.04	7.57	7.17	6.78	6.32	25.18	22.47	20.31	18.23	7.31	14.62	12.68
	MDRL	7.00	6.00	6.00	6.00	6.00	5.00	5.00	18.00	16.00	14.00	13.00	6.00	10.00	9.00
	SDRL	7.01	6.63	6.27	5.82	5.45	5.15	4.73	24.64	22.03	19.69	17.55	5.63	14.04	12.05
1.5	**ARL**	6.00	5.73	5.44	5.23	4.97	4.76	4.46	15.17	13.68	12.33	11.13	5.06	9.06	7.96
	MDRL	5.00	5.00	4.00	4.00	4.00	4.00	4.00	11.00	10.00	9.00	8.00	4.00	6.00	6.00
	SDRL	4.19	3.95	3.70	3.53	3.35	3.15	2.89	14.49	13.06	11.75	10.54	3.41	8.49	7.39
1.75	**ARL**	4.39	4.21	4.03	3.88	3.70	3.55	3.40	9.52	8.65	7.86	7.17	3.76	5.94	5.30
	MDRL	4.00	4.00	3.00	3.00	3.00	3.00	3.00	7.00	6.00	6.00	5.00	3.00	4.00	4.00
	SDRL	2.72	2.58	2.42	2.31	2.18	2.07	1.95	8.95	8.11	7.23	6.62	2.24	5.46	4.80
2	**ARL**	3.42	3.29	3.18	3.08	2.97	2.86	2.75	6.30	5.75	5.25	4.87	3.02	4.14	3.77
	MDRL	3.00	3.00	3.00	3.00	3.00	3.00	2.00	5.00	4.00	4.00	4.00	3.00	3.00	3.00
	SDRL	1.84	1.76	1.69	1.61	1.54	1.48	1.40	5.75	5.21	4.70	4.31	1.58	3.62	3.23
2.5	**ARL**	2.39	2.33	2.26	2.20	2.13	2.08	2.00	3.23	3.03	2.83	2.67	2.16	2.39	2.23
	MDRL	2.00	2.00	2.00	2.00	2.00	2.00	2.00	2.00	2.00	2.00	2.00	2.00	2.00	2.00
	SDRL	1.07	1.05	1.02	1.00	0.97	0.94	0.91	2.65	2.45	2.27	2.11	0.97	1.81	1.64
3	**ARL**	1.85	1.80	1.76	1.71	1.68	1.65	1.60	2.02	1.91	1.83	1.76	1.69	1.63	1.56
	MDRL	2.00	2.00	2.00	2.00	2.00	2.00	2.00	2.00	1.00	1.00	1.00	2.00	1.00	1.00
	SDRL	0.75	0.73	0.72	0.71	0.69	0.68	0.66	1.41	1.31	1.22	1.15	0.69	1.01	0.92
3.5	**ARL**	1.52	1.49	1.46	1.43	1.40	1.37	1.34	1.45	1.41	1.37	1.33	1.41	1.27	1.23
	MDRL	1.00	1.00	1.00	1.00	1.00	1.00	1.00	1.00	1.00	1.00	1.00	1.00	1.00	1.00
	SDRL	0.58	0.58	0.56	0.55	0.54	0.53	0.52	0.80	0.75	0.71	0.66	0.55	0.59	0.54
4	**ARL**	1.30	1.27	1.25	1.23	1.20	1.18	1.16	1.19	1.17	1.15	1.13	1.21	1.10	1.09
	MDRL	1.00	1.00	1.00	1.00	1.00	1.00	1.00	1.00	1.00	1.00	1.00	1.00	1.00	1.00
	SDRL	0.47	0.46	0.44	0.43	0.41	0.39	0.37	0.47	0.44	0.41	0.39	0.42	0.34	0.31

Table 3. ARL performance of EWMA, FIR-EWMA, CUSUM and SEWMA$_{\beta}$ charts when $\lambda = .25$ and $ARL_0 = 168,400, 500$.

	δ								
Control chart	0	0.25	0.5	0.75	1	1.25	1.5	1.75	2
EWMA	167.76	74.89	27.44	13.52	8.21	5.78	4.44	3.62	3.07
CUSUM	167.2	74.31	26.65	13.4	8.37	6.05	4.77	3.35	2.45
SEWMA($\beta = 0.1$)	168.66	68.01	23.59	11.5	7.05	5.05	3.91	3.21	2.76
SEWMA($\beta = 0.125$)	167.9	65.09	23.33	10.91	6.74	4.84	3.78	3.12	2.68
EWMA	400.98	146.32	43.01	18.7	10.5	7.04	5.27	4.19	3.5
CUSUM	402.17	129.87	35.78	16.37	10.06	7.15	5.62	3.9	2.33
SEWMA($\beta = 0.1$)	399.69	123.96	34.77	15.32	8.73	6	4.56	3.86	3.1
SEWMA($\beta = 0.125$)	399.33	116.45	32.28	14.32	8.26	5.71	4.37	3.54	3
EWMA	502.52	171.46	48.66	20.4	11.19	7.39	5.47	4.34	3.62
CUSUM	500	143.87	37.71	17.29	10.53	7.49	5.77	4.04	3.67
SEWMA($\beta = 0.1$)	501.54	147	38.46	16.4	9.19	6.26	4.72	3.77	3.19
SEWMA($\beta = 0.125$)	500.65	135.71	35.34	15.34	8.66	5.95	4.51	3.66	3.08
EWMA	502.52	171.46	48.66	20.4	11.19	7.39	5.47	4.34	3.62
FIR-EWMA	515	169.8	47.6	19.5	10.6	5	3.1	1.7	1.2
SEWMA($\beta = 0.1$)	501.54	147	38.46	16.4	9.19	6.26	4.72	3.77	3.19
SEWMA($\beta = 0.125$)	500.65	135.71	35.34	15.34	8.66	5.95	4.51	3.66	3.08

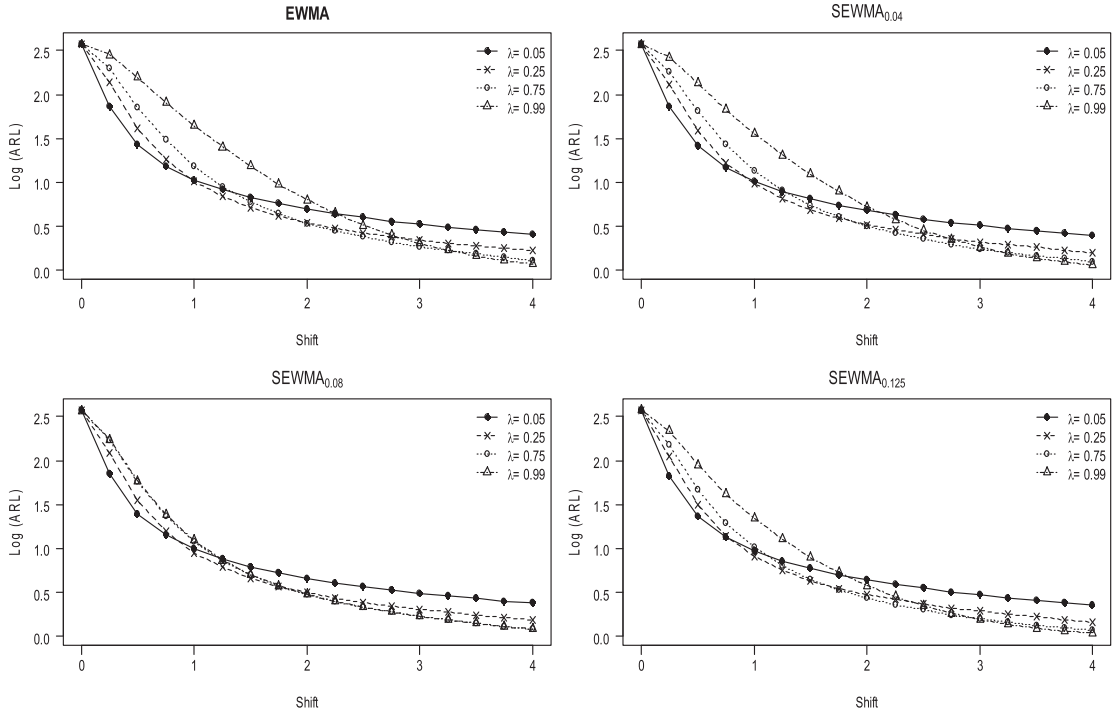

Figure 3. ARL comparison of EWMA and SEWMA$_{\beta}$ charts when $ARL_0 = 370$ and $\lambda = 0.05, 0.25, 0.50$ and 0.99.

ARL values of 147 and135.71, respectively, whereas the same values for CUSUM and EWMA are, respectively, 143.87 and 171.46 at $ARL_0 = 500$ and $\delta = .25$. Similar ARL performance may be observed for $ARL_0 = 168$ and 400.

ii. SEWMA$_{\beta}$ versus FIR-EWMA charts at $ARL_0 = 500$

Table 3 exhibits the comparative *ARL* performance of SEWMA$_{\beta}$ using ($\beta = 10\%$ and 12.5%) versus FIR-EWMA at $ARL_0 = 500$ (cf. [30]). From Table 3, the ARL_1 values for SEWMA$_{\beta}$ $\beta = 10\%$ and 12.5% at $\delta = .25$ are 147.71 and 135.1, respectively. FIR-EWMA exhibits ARL of 47.6 which is smaller than EWMA. Although similar ARL_1 may be observed for other shifts, SEWMA$_{\beta}$ showed better ARL_1 than FIR-EWMA for shifts up to $\delta = 1.5$.

4.2.1. General Comments

The proposed design exhibits better performance than EWMA for all choices of $\beta > 0$. As β increases, the performance of the SEWMA$_{\beta}$ chart becomes increasingly better than EWMA, especially for higher values of smoothing parameter λ (cf. Table 3). The proposed SEWMA$_{\beta}$ chart outperforms the CUSUM chart at all levels of shift δ. The performance of the SEWMA$_{\beta}$ chart (compared with CUSUM chart) gets better with increase in *p*. Table 3 also provides the comparison of SEWMA$_{\beta}$ chart ($\beta = 10\%$ and 12.5%) versus FIR-EWMA at $\lambda = .25$ and $ARL_0 = 500$ [36]. It is noticed that as β increases, SEWMA$_{\beta}$ chart is more sensitive for the detection of shifts as compared with FIR-EWMA chart (cf. last row of Table 3). Overall, **t**he proposed SEWMA$_{\beta}$ chart performs

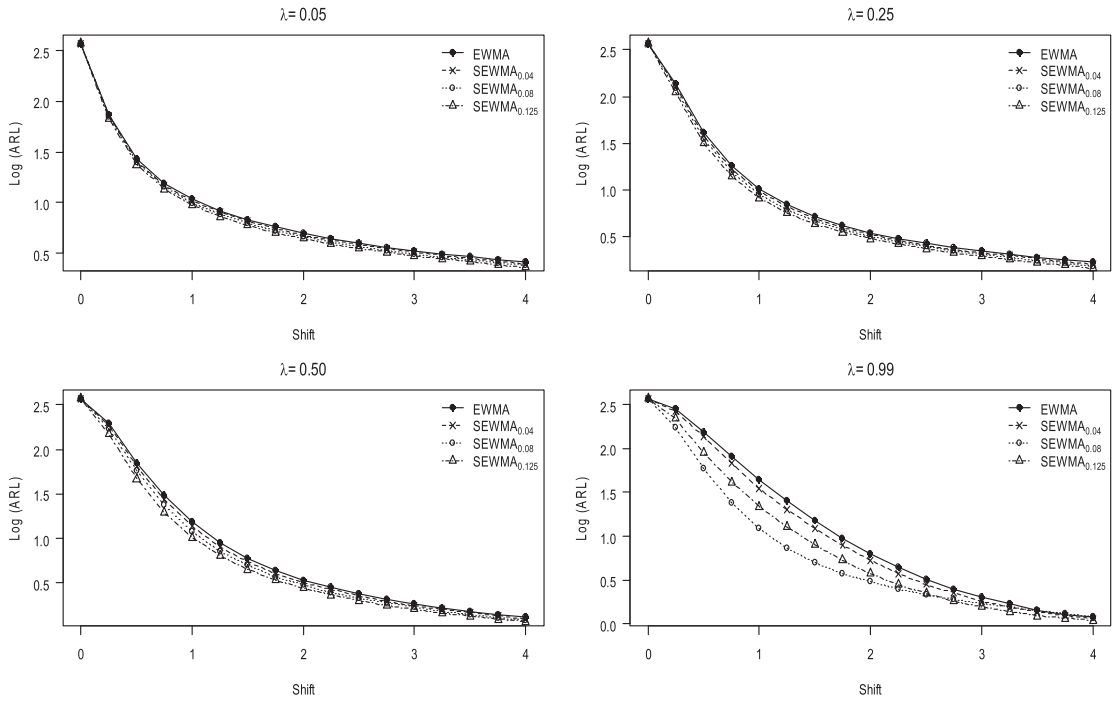

Figure 4. ARL comparison of EWMA and SEWMA$_{\beta}$ charts (at different levels of β) when ARL$_0$ = 370 and λ = 0.05, 0.25, 0.50 and 0.99.

better than other competing charts (such as EWMA, CUSUM and FIR-EWMA charts) for detecting shifts in the process mean level. The performance of the SEWMA$_{\beta}$ chart relies mainly on the choice of λ and β. The detection ability of the SEWMA$_{\beta}$ chart improves with an increase in p at all levels of λ. For a fixed β, if the interest is in the detection of small shifts, it is recommended to use low values ofλ (i.e. λ = 0.05 or 0.25). In the next section, a real-life application for monitoring the strength of steel rods is presented.

It is to be mentioned that the current study is designed under normality; however, one may extend this for other distributional environments such as Maxwell, Weibull, Burr, Power, etc. (cf. Al Mutairi and Volodin [31], Basheer [32], Haq et al. [33], Hossain et al. [34, 35]).

5. A real application of SEWMA$_{\beta}$ to steel rod manufacturing industry

This section presents a real-life application of the proposed technique in a production line that relates to an ongoing monitoring process of steel rod manufacturing. The steel industry is a booming industry and it plays an essential role in the development of a country and helps strengthen the economy. Most of the steel manufactured by an aluminium plant or a steel mill is moulded through extrusion or rolling into long continuous strips of numerous shape and size. Several testing techniques are commercially available and can be customized to meet specific inspection needs. Whether manual, automated or phased array, ultrasonic

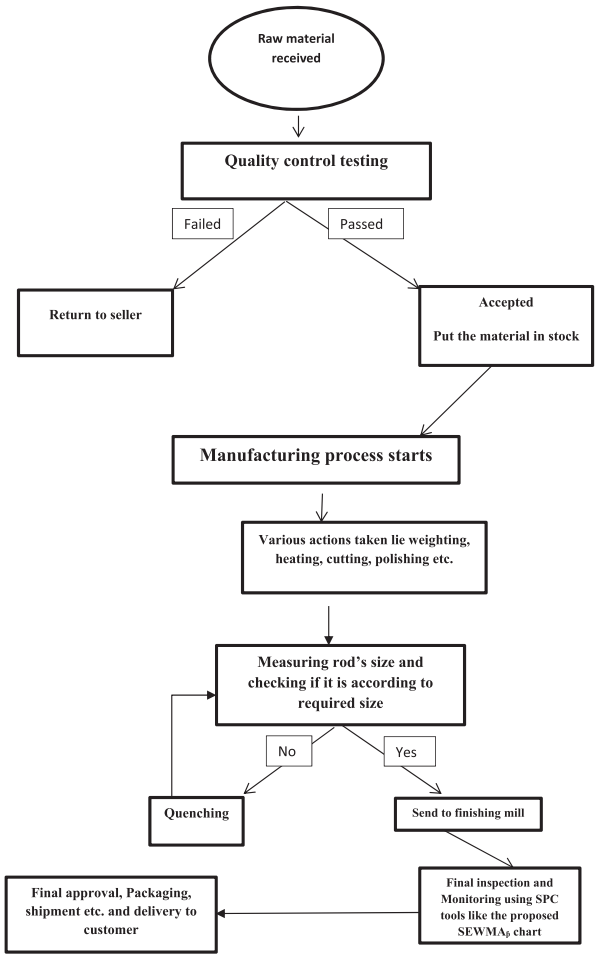

Figure 5. A flow of SEWMA$_{\beta}$ design in steel rod manufacturing process

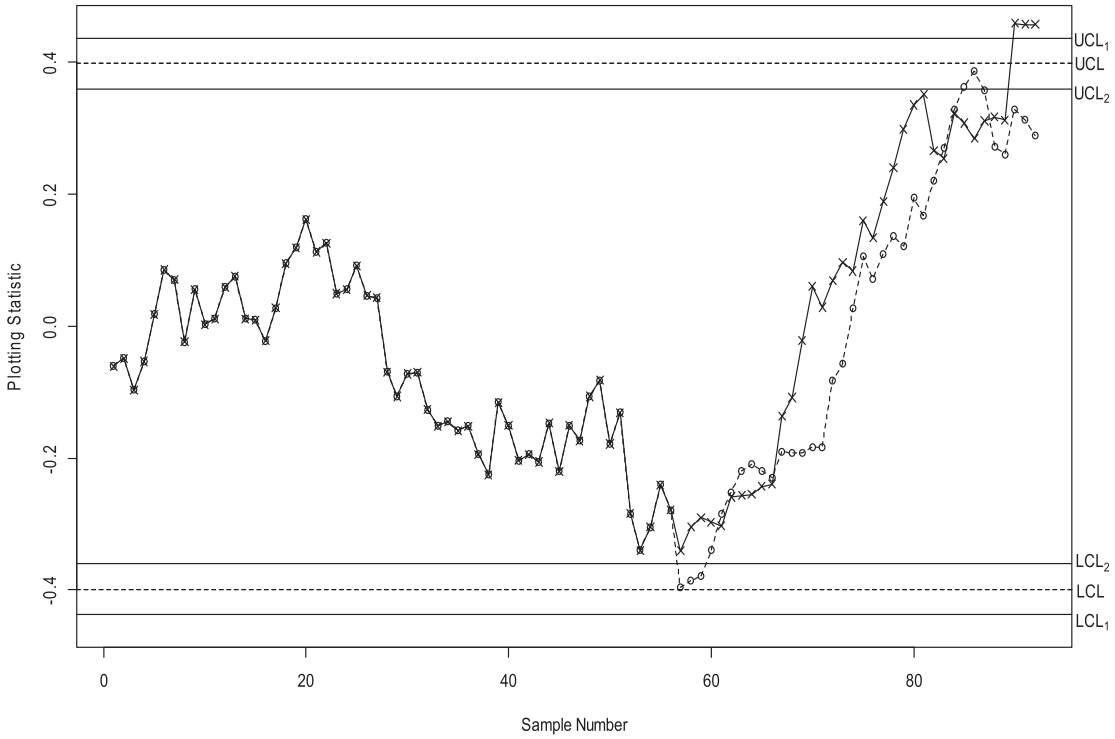

Figure 6. Control charts of the EWMA and SEWMA$_{\beta}$ for the steel rod data when $\lambda = 0.05$ and $\beta = 0.1$.

testing can help manufacturers of bars, tubing and related metal products to assure product quality and customer satisfaction. But without proper SPC techniques, it will be time consuming and costly. To reduce the cost, it is necessary to use such techniques which provide a timely identification of any deviations from the stable state of a process. Several authors designed efficient SPC techniques to identify the unusual variations present during several processes. Lyu and Chen [36] designed a multivariate SPC technique to detect defects which often occur during manufacturing process. Pérez-González et al. [37] applied SPC to get the proper decision from the entire emergency and security system. In several steel manufacturing industries, quality control techniques are implemented to enhance process monitoring of designing and manufacturing steel rods. Christyanti [38], Naeem et al. [39] and the references therein may be seen for further details related to the topic. They used different statistical approaches like DOE (design of experiment) and $\bar{X}$ chart for the identification of special causes. They suggested that 6-sigma procedures really helps to identify the special causes during process monitoring. Figure 5 provides a graphical representation of the monitoring process in steel rod manufacturing, where one can potentially use the proposed SEWMA$_{\beta}$ chart.

The data we have used here is related to the steel manufacturing industry. The breaking strength of the rods is our quality characteristic of interest that needs monitoring over time for a better quality of the products related to the process output. A sample of 90 steel rods measurements is collected from the aforementioned process, and their breaking strength is measured. Through distribution fitting tests, we identified that the breaking strengths of the steel rods follow a normal distribution. We have constructed SEWMA$_{\beta}$ and the classical EWMA charts for this dataset using $\lambda = .05$ and $\beta = 0.1$. Figure 6 presents these comparative charts where UCL and LCL refer to limits of the classical EWMA, while the other two pairs (LCL$_1$, UCL$_1$) and (LCL$_2$, UCL$_2$) correspond to the SEWMA$_{\beta}$ chart. It is observed that the proposed design is not only indicating the shift earlier than the classical EWMA, but it is also giving a larger number of out-of-control signals (this is exactly in accordance with the findings in Section 4).

These earlier and larger detections by SEWMA$_{\beta}$ design has many practical implications for process monitoring. It may be used as a tool needed to reduce the amount of labour and to perform cost-effective experimentations. The potential factors causing out-of-control signals might include changes in these factors: mechanical properties of metal, hardness level, yield strength, intensity of temperature, the grain size, atmospheric pressure, the quality of the protective surface film, the presence of certain agents reducing any corrosive effects, the presence of surface cracks or discontinuities and other environmental condition. These kinds of abnormalities may be identified by using appropriate SPC techniques such as the newly proposed SEWMA$_{\beta}$ chart of this study.

6. Concluding remarks

This study introduces a memory control chart, namely SEWMA$_{\beta}$ chart, for an efficient monitoring of shifts in the process location parameter. The performance of the

proposed design is assessed by using several *RL* properties (such as *ARL*, *MRL* and *SDRL*) at varying values of design parameters λ_g, β, L_1 and L_2. The results advocate that the proposed design provides enhanced *RL* properties as compared with the classical EWMA, CUSUM and FIR-EWMA charts at several *p* values. As *p* increases, the proposed design offers more sensitivity towards shifts in the process mean relative to the competing charts. A real-life application concerning the breaking strength of steel rods highlights the significance of our study.

The current work can be extended to study the performance of CUSUM, mixed / combined Shewhart, EWMA-CUSUM charts both in univariate and multivariate directions for location and dispersion parameters. The scope may further be extended to cover mixed and sequential sampling techniques in SPC for efficient process monitoring of non-normally distributed process.

Acknowledgements

The authors are thankful to the anonymous reviewer for the constructive comments that helped in improving the initial version of the paper. The author Saddam Akber Abbasi would like to acknowledge Qatar University for providing excellent research facilities. The authors, M. Hafidz Omar and Muhammad Riaz, would also like to acknowledge the research facilities provided by the Deanship of Scientific Research (DSR) at King Fahd University of Petroleum & Minerals (KFUPM).

Disclosure statement

No potential conflict of interest was reported by the authors.

ORCID

Saddam Akber Abbasi http://orcid.org/0000-0003-1843-8863
Qurat-Ul-Ain Khaliq http://orcid.org/0000-0002-6562-5787
Muhammad Riaz http://orcid.org/0000-0002-7599-6928

References

[1] Montgomery DC. Introduction to statistical quality control. 7th ed. Hoboken (NJ): John Wiley & Sons; 2013.
[2] Shewhart WA. Quality control charts. Bell Labs Tech J. 1926;5:593–603.
[3] Roberts SW. Control chart tests based on geometric moving averages. Technometrics. 1959;1:239–250.
[4] Page ES. Continuous inspection schemes. Biometrika. 1954;41:100–115.
[5] Yang SF, Lin JS, Cheng SW. A new nonparametric EWMA sign control chart. Expert Syst Appl. 2011;38:6239–6243.
[6] Matheson LA. On sequential versus random sampling in statistical process control. Benchmarking Qual Manag Technol. 1996;3:19–27.
[7] Green RH. Sampling design and statistical methods for environmental biologists. New York (NY): John Wiley & Sons; 1979.
[8] Green RH. On fixed precision level sequential sampling. Res Popul Ecol (Kyoto). 1970;12:249–251.
[9] Stoumbos ZG, Reynolds Jr. MR. Control charts applying a general sequential test at each sampling point. Seq Anal. 1996;15:159–183.
[10] Stoumbos ZG, Reynolds Jr. MR. Control charts applying a sequential test at fixed sampling intervals. J Qual Technol. 1997;29:21–40.
[11] Peng Y, Reynolds Jr. MR. A GLR control chart for monitoring the process mean with sequential sampling. Seq Anal. 2014;33:298–317.
[12] Steiner SH, Geyer PL, Wesolowsky GO. Grouped data-sequential probability ratio tests and cumulative sum control charts. Technometrics. 1996;38:230–237.
[13] Reynolds Jr. MR. Evaluating properties of variable sampling interval control charts. Seq Anal. 1995;14:59–97.
[14] Reynolds Jr. MR. Shewhart and EWMA variable sampling interval control charts with sampling at fixed times. J Qual Technol. 1996a;28:199–212.
[15] Reynolds Jr. MR. Variable sampling interval control charts with sampling at fixed times. IIE Trans. 1996b;28:497–510.
[16] Reynolds Jr. MR, Amin RW, Arnold JC. CUSUM charts with variable sampling intervals. Technometrics. 1990;32:371–384.
[17] Reynolds Jr. MR, Amin RW, Arnold JC, et al. X^2 charts with variable sampling intervals. Technometrics. 1988;30:81–192.
[18] Reynolds Jr. MR, Arnold JC. Optimal one-sided Shewhart control charts with variable sampling intervals. Seq Anal. 1989;8:51–77.
[19] Zhang CW, Xie M, Goh TN. Design of exponential control charts using a sequential sampling scheme. IIE Trans. 2006;38:1105–1116.
[20] Stoumbos ZG, Reynolds Jr. MR. The SPRT control chart for the process mean with samples starting at fixed times. Nonlinear Anal: Real World Appl. 2001;2:1–34.
[21] Ou Y, Wu Z, Chen S, et al. An improved SPRT control chart for monitoring process mean. Int J Adv Manuf Technol. 2010;51:1045–1054.
[22] Ou Y, Wu Z, Yu FJ, et al. An SPRT control chart with variable sampling intervals. Int J Adv Manuf Technol. 2011;56:1149–1158.
[23] Xu S, Jeske DR. Repeated SPRT charts for monitoring INAR (1) processes. Qual Reliab Eng Int. 2017;33:2615–2624.
[24] Godase DG, Mahadik SB. The SPRT control chart for process dispersion. Qual Reliab Eng Int. 2019. doi:10.1002/qre.2481.
[25] Wald A. Sequential tests of statistical hypotheses. Ann Math Stat. 1945;16:117–186.
[26] Chakraborti S. Run length, average run length, and false alarm rate of Shewhart X-bar chart: exact derivations by conditioning. Commun Stat-Simul Comput. 2002;29:61–81.
[27] Khaliq QUA, Riaz M, Alemi F. Performance of Tukey's and individual/moving range control charts. Qual Reliab Eng Int. 2015;31:1063–1077.
[28] Quesenberry CP. The effects of sample size on estimated limits for and X control charts. J Qual Technol. 1993;25:237–247.
[29] Khaliq QUA, Riaz M, Ahmad S. On designing a new Tukey-EWMA control chart for process monitoring. Int J Adv Manuf Technol. 2016;82:1–23.
[30] Steiner SH. EWMA control charts with time-varying control limits and fast initial response. J Qual Technol. 1999;31:75–86.
[31] Al Mutairi AO, Volodin A. Special cases in order statistics for the alternative parametrization of the generalized power function distribution. J Taibah Univer Sci. 2018;12:285–289.
[32] Basheer AM. Alpha power inverse Weibull distribution with reliability application. J Taibah Univer Sci. 2019;13:423–432.

[33] Haq MAU, Elgarhy M, Hashmi S. The generalized odd Burr III family of distributions: properties, applications and characterizations. J Taibah Univer Sci. 2019;13:961–971.
[34] Hossain MP, Omar MH, Riaz M. New V control chart for the Maxwell distribution. J Stat Comput Simul. 2017;87(3):594–606.
[35] Hossain MP, Sanusi RA, Omar MH, et al. On designing Maxwell CUSUM control chart: an efficient way to monitor failure rates in boring processes. Int J Adv Manuf Technol. 2019;100:1923–1930.
[36] Lyu J, Chen M. Automated visual inspection expert system for multivariate statistical process control chart. Expert Syst Appl. 2009;36:5113–5118.
[37] Pérez-González CJ, Colebrook M, Roda-García JL, et al. Developing a data analytics platform to support decision making in emergency and security management. Expert Syst Appl. 2019;120:167–184.
[38] Christyanti J. Improving the quality of asbestos roofing at PT BBI using six sigma methodology. Procedia-Soc Behav Sci. 2012;65:306–312.
[39] Naeem K, Ullah M, Tariq A, et al. Optimization of steel bar manufacturing process using six sigma. Chin J Mech Eng. 2016;29:332–341.
[40] Klugman SA, Panjer HH, Willmot GE. Loss models: from data to decisions. Vol. 715. John Wiley & Sons; 2012.

Appendix

For derivations of some results in this appendix, we will rely on the following Theorem, which we present without proof, on the moments of the random sum of random variables from Klugman et al. (2014)

Theorem 1: *([40], Equation (9.9)). Let the random sum, $S = \sum_{j=1}^{N} X_j$ where X_j is iid from any distribution $f(x;\mu,\sigma^2)$ and the size random variable, N, has a distribution $h(n;m,\pi)$. Then, the first two moments of S are as follows:*

$$E(S)=E(N)E(X) \quad \text{and} \quad \text{Var}(S)=E(N)\,\text{Var}(X)+\text{Var}(N)(E(X))^2.$$

Definition 1: Let us denote R_s as the resampling region. With $0<\lambda_g\leq 1$ and for $j=1,2,3,\ldots,$ the sequential EWMA random variable Z_j is defined as follows $Z_j=\lambda_g I_j+(1-\lambda_g)Z_{j-1}$

$$I_j=\begin{cases} X_j & \text{if } X_j\notin R_s \\ X_j+Y_{j1} & \text{if } Z_{j1}\in R_s \\ X_j+Y_{j1}+Y_{j2} & \text{if } Z_{j2}\in R_s \\ \vdots & \vdots \end{cases} \quad \text{where } E[Z_0]=\mu_0.$$

For compactness, we can alternatively denote I_j as follows:

$$I_j=\begin{cases} X_j & \text{if} X_j\notin R_s \\ X_j+\sum_{k=1}^{N_j} Y_{j,k} & \text{if} Z_j\in R_s. \end{cases}$$

Or alternatively, we can denote I_j as

$$I_j=X_j+\sum_{k=0}^{N_j} Y_{j,k} \text{ where } Y_{j0}=\cdot \text{ when } X_j\notin R_s.$$

We note that the probability of a sample $Z_j\in R_s$ is given by $P(Z_j\in R_s)=\gamma$. We note that the random sample $Y_{j,k}$ will be drawn sequentially at each stage j until $Z_j\notin R_s$. As such, the random variable N_j measures the sample size needed until Z_j is outside of the resampling region. Thus, N_j is a geometrically distributed random variable. We also note that the random sample X_j comes from a normal distribution with a mean of μ_0 and variance of σ_0^2. The sequential random sample $Y_{j,k}$ also comes from a normal distribution with a mean of μ_0 and variance of σ_0^2. For simplicity of derivations and results for the first two centred moments of Z_j, we will use the transformation $\lambda_g^*=1-\lambda_g$.

A) **Derivation of the Mean of Z_j.**

1) Mean of Z_1.

$$\begin{aligned} E[Z_1] &= E[\lambda_g I_1+(1-\lambda_g)Z_0]=E[\lambda_g^* Z_0+(1-\lambda_g^*)I_1] \\ &= E[\lambda_g^* Z_0+(1-\lambda_g^*)I_1]=\lambda_g^* E[Z_0]+(1-\lambda_g^*)E[E[I_1|R_s]] \\ &= \lambda_g^*\mu_0+(1-\lambda_g^*)E\left[E\left[X_1+\sum_{k=0}^{N_1}Y_{1,k}|R_s\right]\right] \\ &= \lambda_g^*\mu_0+(1-\lambda_g^*)E[E[X_1|R_s]]+(1-\lambda_g^*) \\ &\quad \times E\left[E\left[\sum_{k=0}^{N_1}Y_{1,k}|R_s\right]\right] \\ &= \lambda_g^*\mu_0+(1-\lambda_g^*)\mu_0+(1-\lambda_g^*)E\left[\sum_{k=0}^{N_1}E[Y_{1,k}|R_s\right]] \\ &= \mu_0+(1-\lambda_g^*)E[N_1]E[Y_{1,k}] \end{aligned}$$

due to Theorem 1 (by Klugman et al.)[41] where $N_1\sim geom(1-\gamma)$ and $Y_{1,k}$ is iid with μ_0. Thus

$$\begin{aligned} E[Z_1] &= \mu_0+(1-\lambda_g^*)\left(\frac{1}{1-\gamma}\right)\mu_0 \\ &= \mu_0\left(1+\frac{1-\lambda_g^*}{1-\gamma}\right). \end{aligned}$$

2) Mean of Z_2.

$$\begin{aligned} E[Z_2] &= E[\lambda_g^* Z_1+(1-\lambda_g^*)I_2]=\lambda_g^* E[Z_1]+(1-\lambda_g^*)E[E[I_2|R_s]] \\ &= \lambda_g^*\mu_0\left(1+\frac{1-\lambda_g^*}{1-\gamma}\right)+(1-\lambda_g^*) \\ &\quad \times E\left[E\left[X_2+\sum_{k=0}^{N_2}Y_{2,k}|R_s\right]\right] \\ &= \lambda_g^*\mu_0+(1-\lambda_g^*)\mu_0+\mu_0\lambda_g^*\left(\frac{1-\lambda_g^*}{1-\gamma}\right) \\ &\quad +(1-\lambda_g^*)E\left[\sum_{k=0}^{N_2}E[Y_{2,k}|R_s\right]] \\ &= \mu_0+\mu_0\lambda_g^*\left(\frac{1-\lambda_g^*}{1-\gamma}\right)+(1-\lambda_g^*)E[N_2]E[Y_{2,k}] \end{aligned}$$

due to Theorem 1 (by Klugman et al.)[41] where $N_2\sim geom(1-\gamma)$ and $Y_{2,k}$ is iid with μ_0. Thus

$$\begin{aligned} E[Z_2] &= \mu_0+\mu_0\lambda_g^*\left(\frac{1-\lambda_g^*}{1-\gamma}\right)+(1-\lambda_g^*)\left(\frac{1}{1-\gamma}\right) \\ \mu_0 &= \mu_0\left(1+\frac{1-\lambda_g^*}{1-\gamma}(\lambda_g^*+1)\right) \\ &= \mu_0\left(1+\frac{(1-\lambda_g^*)(1+\lambda_g^*)}{1-\gamma}\right). \end{aligned}$$

3) Mean of Z_3.

$$E[Z_3]=E[\lambda_g^* Z_2+(1-\lambda_g^*)I_3]=\lambda_g^* E[Z_2]+(1-\lambda_g^*)E[E[I_3|R_s]].$$

By applying Theorem 1 (Klugman et al.)[41] with simplification steps similar to the derivation of $E[Z_2]$, we have,

$$\begin{aligned} E[Z_3] &= \mu_0+\mu_0\lambda_g^*\frac{(1-\lambda_g^*)(1+\lambda_g^*)}{1-\gamma}+(1-\lambda_g^*)\left(\frac{1}{1-\gamma}\right)\mu_0 \\ &= \mu_0\left(1+\frac{(1-\lambda_g^*)}{1-\gamma}(1+\lambda_g^*+\lambda_g^{*2})\right). \end{aligned}$$

4) Mean of Z_4.

$$E[Z_4] = E[\lambda_g^* Z_3 + (1-\lambda_g^*)I_4] = \lambda_g^* E[Z_3] + (1-\lambda_g^*)E[E[I_4|R_s]]$$

By applying Theorem 1 (Klugman et al.)[41] with simplification steps similar to the derivation of $E[Z_3]$, we have,

$$\begin{aligned} E[Z_4] &= \mu_0 + \mu_0 \frac{(1-\lambda_g^*)}{1-\gamma}\lambda_g^*(1+\lambda_g^*+\lambda_g^{*2}) \\ &\quad + (1-\lambda_g^*)\left(\frac{1}{1-\gamma}\right)\mu_0 \\ &= \mu_0\left(1+\frac{(1-\lambda_g^*)}{1-\gamma}(1+\lambda_g^*+\lambda_g^{*2}+\lambda_g^{*3})\right). \end{aligned}$$

5) Mean of Z_j.
The following summarizes the results, we have thus far:

$$\begin{aligned} E[Z_1] &= \mu_0\left(1+\frac{1-\lambda_g^*}{1-\gamma}\right), \\ E[Z_2] &= \mu_0\left(1+\frac{(1-\lambda_g^*)(1+\lambda_g^*)}{1-\gamma}\right), \\ E[Z_3] &= \mu_0\left(1+\frac{(1-\lambda_g^*)}{1-\gamma}(1+\lambda_g^*+\lambda_g^{*2})\right), \text{ and} \\ E[Z_4] &= \mu_0\left(1+\frac{(1-\lambda_g^*)}{1-\gamma}(1+\lambda_g^*+\lambda_g^{*2}+\lambda_g^{*3})\right). \end{aligned}$$

Based on these, we now let

$$E[Z_{j-1}] = \mu_0\left(1+\frac{(1-\lambda_g^*)}{1-\gamma}\sum_{k=0}^{j-2}\lambda_g^{*k}\right).$$

Then by induction, we have

$$\begin{aligned} E[Z_j] &= E[\lambda_g^* Z_{j-1} + (1-\lambda_g^*)I_j] \\ &= \lambda_g^* E[Z_{j-1}] + (1-\lambda_g^*)E[E[I_j|R_s]] \\ &= \lambda_g^*\mu_0\left(1+\frac{(1-\lambda_g^*)}{1-\gamma}\sum_{k=0}^{j-2}\lambda_g^{*k}\right) \\ &\quad + (1-\lambda_g^*)E\left[E\left[X_j+\sum_{k=0}^{N_j}Y_{j,k}|R_s\right]\right] \\ &= \lambda_g^*\mu_0 + (1-\lambda_g^*)E[E[X_j|R_s]] + \mu_0\frac{(1-\lambda_g^*)}{1-\gamma}\lambda_g^*\sum_{k=0}^{j-2}\lambda_g^{*k} \\ &\quad + (1-\lambda_g^*)E\left[E\left[\sum_{k=0}^{N_j}Y_{j,k}|R_s\right]\right] \\ &= \lambda_g^*\mu_0 + (1-\lambda_g^*)\mu_0 + \mu_0\frac{(1-\lambda_g^*)}{1-\gamma}\sum_{k=0}^{j-2}\lambda_g^{*k+1} \\ &\quad + (1-\lambda_g^*)E\left[\sum_{k=0}^{N_j}E[Y_{j,k}|R_s]\right] \\ &= \mu_0 + \mu_0\frac{(1-\lambda_g^*)}{1-\gamma}\sum_{k=0}^{j-2}\lambda_g^{*k+1} + (1-\lambda_g^*)E[N_j]E[Y_{j,k}] \end{aligned}$$

due to Theorem 1 (by Klugman et al.)[41] where $N_j \sim geom(1-\gamma)$ and $Y_{j,k}$ is iid with μ_0. Thus,

$$\begin{aligned} E[Z_j] &= \mu_0 + \mu_0\frac{(1-\lambda_g^*)}{1-\gamma}\sum_{k=0}^{j-2}\lambda_g^{*k+1} + (1-\lambda_g^*)\left(\frac{1}{1-\gamma}\right)\mu_0 \\ &= \mu_0\left(1+\frac{1-\lambda_g^*}{1-\gamma}\left(\sum_{k=0}^{j-2}\lambda_g^{*k+1}+1\right)\right) \\ &= \mu_0\left(1+\frac{(1-\lambda_g^*)}{1-\gamma}\sum_{m=0}^{j-1}\lambda_g^{*m}\right). \end{aligned}$$

Since $0 < \lambda_g^* < 1$, we can also reexpress the above as follows:

$$\begin{aligned} E[Z_j] &= \mu_0\left(1+\frac{(1-\lambda_g^*)}{1-\gamma}\sum_{m=0}^{j-1}\lambda_g^{*m}\right) \\ &= \mu_0\left(1+\frac{(1-\lambda_g^*)}{1-\gamma}\frac{(1-\lambda_g^{*j})}{1-\lambda_g^*}\right) \\ &= \mu_0\left(1+\frac{1-\lambda_g^{*j}}{1-\gamma}\right). \end{aligned}$$

B) Asymptotic behaviour of the mean of Z_j.

Since $0 < \lambda_g^* < 1$, as j grows large, we have the following:

$$\begin{aligned} \lim_{j\to\infty} E[Z_j] &= \lim_{j\to\infty}\mu_0\left(1+\frac{1-\lambda_g^{*j}}{1-\gamma}\right) = \mu_0\left(1+\lim_{j\to\infty}\frac{1-\lambda_g^{*j}}{1-\gamma}\right) \\ &= \mu_0\left(1+\frac{1-\lim_{j\to\infty}\lambda_g^{*j}}{1-\gamma}\right) = \mu_0\left(1+\frac{1}{1-\gamma}\right). \end{aligned}$$

C) Derivation of the variance of Z_j.

1) Variance of Z_1.

$$\begin{aligned} \mathrm{Var}[Z_1] &= \mathrm{Var}[\lambda_g I_1 + (1-\lambda_g)Z_0] = \mathrm{Var}[\lambda_g^* Z_0 + (1-\lambda_g^*)I_1] \\ &= \lambda_g^{*2}\mathrm{Var}[Z_0] + (1-\lambda_g^*)^2\mathrm{Var}(I_1) \text{ since } \mathrm{Cov}(Z_0, I_1) = 0 \\ &= \lambda_g^{*2}\sigma_0^2 + (1-\lambda_g^*)^2\mathrm{Var}\left(X_1+\sum_{k=0}^{N_1}Y_{1,k}\right) \\ &= \lambda_g^{*2}\sigma_0^2 + (1-\lambda_g^*)^2\left(\mathrm{Var}(X_1)+\mathrm{Var}\left(\sum_{k=0}^{N_1}Y_{1,k}\right)\right) \\ &\quad \times \text{since } \mathrm{Cov}(X_1, Y_{1,k}) = 0 \\ &= \lambda_g^{*2}\sigma_0^2 + (1-\lambda_g^*)^2\sigma_0^2 + (1-\lambda_g^*)^2(E(N_1)\mathrm{Var}(Y_{1,k}) \\ &\quad + \mathrm{Var}(N_1)(E(Y_{1,k}))^2) \end{aligned}$$

due to Theorem 1 (by Klugman et al.)[41] where $N_1 \sim geom(1-\gamma)$ and $Y_{1,k}$ is iid with mean μ_0 and variance σ_0^2. Thus,

$$\begin{aligned} \mathrm{Var}[Z_1] &= (\lambda_g^{*2} + (1-\lambda_g^*)^2)\sigma_0^2 + (1-\lambda_g^*)^2 \\ &\quad \left(\left(\frac{1}{1-\gamma}\right)\sigma_0^2 + \frac{\gamma}{(1-\gamma)^2}(\mu_0)^2\right) \\ &= \left(\lambda_g^{*2} + (1-\lambda_g^*)^2\left(1+\frac{1}{1-\gamma}\right)\right)\sigma_0^2 \\ &\quad + \frac{\gamma(1-\lambda_g^*)^2}{(1-\gamma)^2}\mu_0^2. \end{aligned}$$

2) Variance of Z_2.

$$\begin{aligned}\mathrm{Var}[Z_2] &= \mathrm{Var}[\lambda_g I_2 + (1-\lambda_g)Z_1] = \mathrm{Var}[\lambda_g^* Z_1 + (1-\lambda_g^*)I_2] \\ &= \lambda_g^{*2}\mathrm{Var}[Z_1] + (1-\lambda_g^*)^2\mathrm{Var}(I_2) \text{ since } \mathrm{Cov}(Z_1, I_2) = 0 \\ &= \lambda_g^{*2}\mathrm{Var}[Z_1] + (1-\lambda_g^*)^2\mathrm{Var}\left(X_2 + \sum_{k=0}^{N_2} Y_{2,k}\right) \\ &= \left(\lambda_g^{*4} + \lambda_g^{*2}(1-\lambda_g^*)^2\left(1+\frac{1}{1-\gamma}\right)\right)\sigma_0^2 \\ &\quad + \frac{\gamma\lambda_g^{*2}(1-\lambda_g^*)^2}{(1-\gamma)^2}\mu_0^2 \\ &\quad + (1-\lambda_g^*)^2\left(\mathrm{Var}(X_2) + \mathrm{Var}\left(\sum_{k=0}^{N_2} Y_{2,k}\right)\right) \\ &\quad \text{since } \mathrm{Cov}(X_2, Y_{2,k}) = 0 \\ &= \left(\lambda_g^{*4} + \lambda_g^{*2}(1-\lambda_g^*)^2\left(1+\frac{1}{1-\gamma}\right)\right) \\ &\quad \times \sigma_0^2 + \frac{\gamma\lambda_g^{*2}(1-\lambda_g^*)^2}{(1-\gamma)^2}\mu_0^2 \\ &\quad + (1-\lambda_g^*)^2\sigma_0^2 + (1-\lambda_g^*)^2 \\ &\quad \times (E(N_2)\mathrm{Var}(Y_{2,k}) + \mathrm{Var}(N_2)(E(Y_{2,k}))^2)\end{aligned}$$

due to Theorem 1 (by Klugman et al.)[41] where $N_2 \sim geom(1-\gamma)$ and $Y_{2,k}$ is iid with mean μ_0 and variance σ_0^2. Thus,

$$\begin{aligned}\mathrm{Var}[Z_2] &= \left(\lambda_g^{*4} + \lambda_g^{*2}(1-\lambda_g^*)^2\left(1+\frac{1}{1-\gamma}\right) + (1-\lambda_g^*)^2\right) \\ &\quad \times \sigma_0^2 + \frac{\gamma\lambda_g^{*2}(1-\lambda_g^*)^2}{(1-\gamma)^2}\mu_0^2 \\ &\quad + (1-\lambda_g^*)^2\left(\left(\frac{1}{1-\gamma}\right)\sigma_0^2 + \frac{\gamma}{(1-\gamma)^2}(\mu_0)^2\right) \\ &= \left(\lambda_g^{*4} + (1-\lambda_g^*)^2\left(1+\frac{1}{1-\gamma}\right)(1+\lambda_g^{*2})\right)\sigma_0^2 \\ &\quad + \frac{\gamma}{(1-\gamma)^2}(1-\lambda_g^*)^2(1+\lambda_g^{*2})\mu_0^2.\end{aligned}$$

3) Variance of Z_3.

$$\mathrm{Var}[Z_3] = \mathrm{Var}[\lambda_g I_3 + (1-\lambda_g)Z_2] = \mathrm{Var}[\lambda_g^* Z_2 + (1-\lambda_g^*)I_3]$$

With the independence of Z_2 and I_3 and independence of X_3 and $Y_{3,k}$ and by applying Theorem 1 (Klugman et al.)[41] with simplification steps similar to the derivation of $\mathrm{Var}[Z_2]$, we have,

$$\begin{aligned}\mathrm{Var}[Z_3] &= \left(\lambda_g^{*6} + (1-\lambda_g^*)^2\left(1+\frac{1}{1-\gamma}\right)(1+\lambda_g^{*2}(1+\lambda_g^{*2}))\right) \\ &\quad \times \sigma_0^2 + \frac{\gamma}{(1-\gamma)^2}(1-\lambda_g^*)^2(1+\lambda_g^{*2}(1+\lambda_g^{*2}))\mu_0^2.\end{aligned}$$

4) Variance of Z_j.

We now summarize the following results:

$$\begin{aligned}\mathrm{Var}[Z_1] &= \left(\lambda_g^{*2} + (1-\lambda_g^*)^2\left(1+\frac{1}{1-\gamma}\right)\right) \\ &\quad \times \sigma_0^2 + \frac{\gamma(1-\lambda_g^*)^2}{(1-\gamma)^2}\mu_0^2,\end{aligned}$$

$$\begin{aligned}\mathrm{Var}[Z_2] &= \left(\lambda_g^{*4} + (1-\lambda_g^*)^2\left(1+\frac{1}{1-\gamma}\right)(1+\lambda_g^{*2})\right) \\ &\quad \times \sigma_0^2 + \frac{\gamma}{(1-\gamma)^2}(1-\lambda_g^*)^2(1+\lambda_g^{*2})\mu_0^2, \text{ and} \\ \mathrm{Var}[Z_3] &= \left(\lambda_g^{*6} + (1-\lambda_g^*)^2\left(1+\frac{1}{1-\gamma}\right)(1+\lambda_g^{*2}(1+\lambda_g^{*2}))\right) \\ &\quad \times \sigma_0^2 + \frac{\gamma}{(1-\gamma)^2}(1-\lambda_g^*)^2(1+\lambda_g^{*2}(1+\lambda_g^{*2}))\mu_0^2.\end{aligned}$$

Based on the above, we now let

$$\begin{aligned}\mathrm{Var}[Z_{j-1}] &= \left(\lambda_g^{*2(j-1)} + (1-\lambda_g^*)^2\left(1+\frac{1}{1-\gamma}\right)\sum_{k=0}^{j-2}\lambda_g^{*2k}\right) \\ &\quad \times \sigma_0^2 + \frac{\gamma}{(1-\gamma)^2}(1-\lambda_g^*)^2\mu_0^2\sum_{k=0}^{j-2}\lambda_g^{*2k}.\end{aligned}$$

Then by induction, we have

$$\begin{aligned}\mathrm{Var}[Z_j] &= \mathrm{Var}[\lambda_g I_j + (1-\lambda_g)Z_{j-1}] = \mathrm{Var}[\lambda_g^* Z_{j-1} + (1-\lambda_g^*)I_j] \\ &= \lambda_g^{*2}Var[Z_{j-1}] + (1-\lambda_g^*)^2 \\ &\quad \mathrm{Var}(I_j) \text{ since } \mathrm{Cov}(Z_{j-1}, I_j) = 0 \\ &= \lambda_g^{*2}Var[Z_{j-1}] + (1-\lambda_g^*)^2 Var\left(X_j + \sum_{k=0}^{N_j} Y_{j,k}\right) \\ &= \left(\lambda_g^{*2j} + (1-\lambda_g^*)^2\left(1+\frac{1}{1-\gamma}\right)\lambda_g^{*2}\sum_{k=0}^{j-2}\lambda_g^{*2k}\right) \\ &\quad \times \sigma_0^2 + \frac{\gamma}{(1-\gamma)^2}(1-\lambda_g^*)^2\mu_0^2\sum_{k=0}^{j-2}\lambda_g^{*2(k+1)} \\ &\quad + (1-\lambda_g^*)^2\sigma_0^2 \\ &\quad + (1-\lambda_g^*)^2(E(N_j)\mathrm{Var}(Y_{j,k}) + \mathrm{Var}(N_j)(E(Y_{j,k}))^2)\end{aligned}$$

due to Theorem 1 (Klugman et al.)[41] where $N_j \sim geom(1-\gamma)$ and $Y_{j,k}$ is iid with mean μ_0 and variance σ_0^2. Thus,

$$\begin{aligned}\mathrm{Var}[Z_j] &= \left(\lambda_g^{*2j} + (1-\lambda_g^*)^2\left(1+\frac{1}{1-\gamma}\right)\right. \\ &\quad \left.\sum_{k=0}^{j-2}\lambda_g^{*2(k+1)} + (1-\lambda_g^*)^2\right) \\ &\quad \times \sigma_0^2 + \frac{\mu_0^2\gamma}{(1-\gamma)^2}(1-\lambda_g^*)^2\sum_{k=0}^{j-2}\lambda_g^{*2(k+1)} + (1-\lambda_g^*)^2 \\ &\quad \times \left(\left(\frac{1}{1-\gamma}\right)\sigma_0^2 + \frac{\gamma}{(1-\gamma)^2}(\mu_0)^2\right) \\ &= \left(\lambda_g^{*2j} + (1-\lambda_g^*)^2\left(1+\sum_{k=0}^{j-2}\lambda_g^{*2(k+1)}\right)\left(1+\frac{1}{1-\gamma}\right)\right) \\ &\quad \times \sigma_0^2 + \frac{\gamma}{(1-\gamma)^2}(1-\lambda_g^*)^2\left(1+\sum_{k=0}^{j-2}\lambda_g^{*2(k+1)}\right)\mu_0^2 \\ &= \left(\lambda_g^{*2j} + (1-\lambda_g^*)^2\left(1+\frac{1}{1-\gamma}\right)\left(\sum_{m=0}^{j-1}\lambda_g^{*2m}\right)\right) \\ &\quad \times \sigma_0^2 + \frac{\gamma}{(1-\gamma)^2}(1-\lambda_g^*)^2\left(\sum_{m=0}^{j-1}\lambda_g^{*2m}\right)\mu_0^2.\end{aligned}$$

Since $0 < \lambda_g^{*2} \leq 1$, we can also reexpress the above as follows:

$$\mathrm{Var}[Z_j] = \left(\lambda_g^{*2j} + (1-\lambda_g^*)^2 \left(\frac{1-\lambda_g^{*2j}}{1-\lambda_g^{*2}}\right)\left(1+\frac{1}{1-\gamma}\right)\right) \times \sigma_0^2 + \frac{\gamma}{(1-\gamma)^2}(1-\lambda_g^*)^2 \left(\frac{1-\lambda_g^{*2j}}{1-\lambda_g^{*2}}\right)\mu_0^2.$$

D) Asymptotic behaviour of the variance of Z_j.

Since $0 < \lambda_g^* \leq 1$, as j grows large we have the following:

$$\lim_{j\to\infty} \mathrm{Var}[Z_j] = \lim_{j\to\infty}\left(\lambda_g^{*2j} + \left(1+\frac{1}{1-\gamma}\right)(1-\lambda_g^*)^2\left(\frac{1-\lambda_g^{*2j}}{1-\lambda_g^{*2}}\right)\right) \times \sigma_0^2 + \lim_{j\to\infty}\frac{\gamma}{(1-\gamma)^2}(1-\lambda_g^*)^2\left(\frac{1-\lambda_g^{*2j}}{1-\lambda_g^{*2}}\right)\mu_0^2$$

$$= \sigma_0^2 \lim_{j\to\infty}(\lambda_g^{*2j}) + \sigma_0^2\left(\left(1+\frac{1}{1-\gamma}\right)\lim_{j\to\infty}(1-\lambda_g^*)^2 \times \left(\frac{1-\lambda_g^{*2j}}{(1+\lambda_g^*)(1-\lambda_g^*)}\right)\right) + \frac{\gamma}{(1-\gamma)^2}(1-\lambda_g^*)^2\left(\frac{1-\lim_{j\to\infty}\lambda_g^{*2j}}{(1+\lambda_g^*)(1-\lambda_g^*)}\right)\mu_0^2$$

$$= \left(1+\frac{1}{1-\gamma}\right)\left(\frac{1-\lambda_g^*}{1+\lambda_g^*}\right)\sigma_0^2 + \frac{\gamma}{(1-\gamma)^2}\left(\frac{1-\lambda_g^*}{1+\lambda_g^*}\right)\mu_0^2.$$